

SELF-INDUCED TRANSPARENCY BY PULSED COHERENT LIGHT*

S. L. McCall† and E. L. Hahn‡

Department of Physics, University of California, Berkeley, California

(Received 10 April 1967)

A nonlinear optical propagation effect¹ has been found in which a short pulse of coherent light above a critical input energy, for a given pulse width τ_p , can pass through an optically resonant medium as though it were transparent; but below the critical energy the pulse energy is absorbed. For times τ_p short compared to T_2' , the inverse of the homogeneous broadening contribution to the optical linewidth $1/T_2$, the effect implies that optical transmission of coherent pulses can be enhanced in a dissipative medium over that of incoherent pulses. The basic propagation effect can be analyzed in the limit of a coherent plane wave, taken, for example, to be circularly polarized:

$$\vec{E}(z, t) = \mathcal{E}(z, t)[\hat{i} \cos(\omega t - kz) - \hat{j} \sin(\omega t - kz)], \quad (1)$$

where the electric field \vec{E} propagates in the z direction with frequency ω , $k = 2\pi\eta/\lambda$, λ is the vacuum wavelength, and η is the constant host-medium refractive index. $\mathcal{E}(z, t)$ is assumed slowly varying so that

$$\frac{\partial \mathcal{E}}{\partial z} \ll \frac{\mathcal{E}}{\lambda} \quad \text{and} \quad \frac{\partial \mathcal{E}}{\partial t} \ll \omega \mathcal{E}.$$

Let N solute ions per cm^3 in the optical ground state present a two-level, inhomogeneously broadened symmetric spectral distribution function $g(\Delta\omega)$ to the driving pulse; and let the center of the spectrum be tuned to frequency ω , with ions at transition frequency ω_0 defined off resonance by amount $\Delta\omega = \omega_0 - \omega$. The condition $\omega^{-1} \ll T_2^* \ll \tau_p \ll T_2'$ is assumed, where $T_2^* \approx g(0)$ is the inverse inhomogeneously broadened linewidth caused by a spread of local static crystalline fields, and $1/T_2 \sim 1/T_2' + 1/T_2^*$. In the language of magnetic resonance, the two-level system can be represented² by an effective macroscopic electric dipole moment $\vec{P} = \hat{u}_0 \mu + \hat{v}_0 v - \hat{w}_0 W \kappa / \omega$, where \hat{u}_0 , \hat{v}_0 , and \hat{w}_0 are orthogonal unit vectors in the fictitious reference frame rotating at frequency ω about the \hat{w}_0 direction. At a particular $\Delta\omega$, \vec{P} is described by the equation

$$d\vec{P}/dt = \vec{P} \times (\hat{u}_0 \kappa \mathcal{E} + \hat{w}_0 \Delta\omega). \quad (2)$$

In the undamped Bloch-equation³ notation, electric dipole absorption (v) and dispersion (u)

components combine with a third component $-\kappa W/\omega$ (in place of M_z), where W is the ion-energy spectral density per cm^3 , $\kappa = 2p/\hbar$, and p is the x or y component of the electric dipole moment of the transition.⁴ After any pulse, the vector \vec{P} with $\Delta\omega = 0$ is turned through a net angle

$$\theta = \kappa \int_{-\infty}^{\infty} \mathcal{E}(z, t) dt. \quad (3)$$

However, $\mathcal{E}(z, t)$ is determined by its initial form at $z = 0$, and by the superposition of all the dipole sources throughout the spectrum, as seen from the reduced Maxwell equation for the forward traveling wave:

$$\begin{aligned} \frac{\partial \mathcal{E}(z, t)}{\partial z} + \frac{\eta}{c} \frac{\partial \mathcal{E}(z, t)}{\partial t} \\ = \frac{-2\pi\omega}{\eta c} \int_{-\infty}^{\infty} g(\Delta\omega) v(z, t, \Delta\omega) d(\Delta\omega), \end{aligned} \quad (4)$$

where c is the speed of light in vacuum, $\int_{-\infty}^{\infty} g(\Delta\omega) \times d(\Delta\omega) = 1$, and $|\partial \vec{P} / \partial t| \ll \omega |\vec{P}|$. For weak pulses of coherent or incoherent light which do not significantly alter the ground-state population, the decay in intensity at frequency ω is given by

$$\mathcal{E}^2(z) = \mathcal{E}^2(0) e^{-\alpha z}, \quad (5)$$

where $\alpha = 8\pi^2 p^2 \omega g(0) N / \eta \hbar c$. Upon coupling Eq. (2) with (3) and (4) we obtain, for large coherent light intensities,

$$\frac{d\theta}{dz} = -\frac{\alpha}{2} \sin\theta, \quad (6)$$

which has the solution

$$\tan \frac{1}{2} \theta(z) = (\tan \frac{1}{2} \theta_0) \exp(-\frac{1}{2} \alpha z). \quad (7)$$

Equation (5) follows from Eq. (7) in the limit of small θ . Here θ_0 is the rotation angle for those ions with $\Delta\omega = 0$ at $z = 0$, the entry face plane of the medium.

The branch solutions of θ vs z from Eq. (7) are plotted in Fig. 1(a). Examples of computer plots for \mathcal{E} vs z and t are shown in Fig. 1(b) for cases $\theta_0 = 0.9\pi$ and $\theta_0 = 1.1\pi$. For initial pulse areas $\theta_0 < \pi$, below the critical area at $\theta_0 = \pi$, the pulse area diminishes toward $\theta(z) = 0$ for increasing z in Fig. 1(a), as shown for $\theta_0 = 0.9\pi$ in Fig. 1(b). Above the critical area,

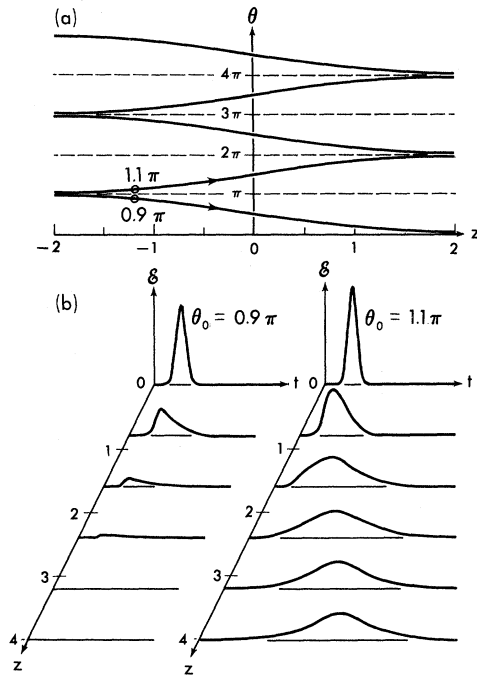


FIG. 1. (a) Branch solutions of θ vs z with formal origin at $z=0$. For a given θ_0 the medium-entry plane is assigned the corresponding z which defines $z=0$ in Eq. (1). For the sample initially in the excited state, θ evolves in the $-z$ direction. Units of z are multiples of $\pi\alpha^{-1}$. (b) Computer plots of \mathcal{E} vs z and t for $\theta_0 = 0.9\pi$ and $\theta_0 = 1.1\pi$ with arbitrary pulse widths. Initial shapes are chosen to be Gaussian. The unit of time is conveniently chosen in terms of input pulse width $\sim\tau_p$. For fixed θ_0 , units of \mathcal{E} are determined from Eq. (3). Units of z are multiples of $\pi\alpha^{-1}$.

a $\theta_0 = 1.1\pi$ pulse increases in area [$\theta(z) \sim \int \mathcal{E} dt$] toward the limit 2π , when $d\theta/dz = 0$. During this process the pulse loses some energy ($\sim \int \mathcal{E}^2 dt$) over a number of absorption lengths α^{-1} and is reshaped. The 2π pulse formed appears to be the traveling wave pulse given by

$$\mathcal{E}(z, t) = \frac{2}{\kappa\tau} \operatorname{sech}\left[\frac{1}{\tau}\left(t - \frac{z}{V}\right)\right], \quad (8)$$

unique in that it represents the only finite-energy pulse solution to Eq. (4) which is unattenuated and retains its shape.⁵ The induced polarization radiates in such a way as to produce the same field pulse given above. V is the pulse velocity and τ is the final pulse width. The final pulse energy in this undamped model is conserved because any optical ion, independent of its assigned $\Delta\omega$, is momentarily excited from its ground state to a coherent superposition of ground and excited states, and then is returned

completely to the ground state after the pulse has gone by. Pulse retardation occurs because the pulse is depleted in energy at its leading time edge during absorption, but the absorbed energy is returned to the lagging edge during emission. Computer calculations show that a given arbitrary input pulse with $\theta_0 \sim 2\pi n$ divides into n separate 2π pulses of the shape given by Eq. (8), after traversing some distance into the medium.

The solution⁶ to the coupled equations (2) and (4) for a pulse of the form (8) may be found without the assumption that $T_2^* \ll \tau_p$. The components of \vec{P} are

$$\begin{aligned} v(\Delta\omega, z, t) &= \frac{Np \sin\varphi}{1 + (\Delta\omega\tau)^2}, \\ u(\Delta\omega, z, t) &= \frac{2Np\Delta\omega\tau \sin\frac{1}{2}\varphi}{1 + (\Delta\omega\tau)^2}, \\ \frac{\kappa}{\omega} W(\Delta\omega, z, t) &= \frac{N\hbar\omega}{2} \left[\frac{2 \sin^2\frac{1}{2}\varphi}{1 + (\Delta\omega\tau)^2} - 1 \right] \frac{\kappa}{\omega} \end{aligned} \quad (9)$$

with

$$\varphi = \kappa \int_{-\infty}^t \mathcal{E}(z, t) dt = 4 \tan^{-1} \left\{ \exp\left[\frac{1}{\tau}\left(t - \frac{z}{V}\right)\right] \right\}.$$

The reciprocal pulse velocity is found to be

$$V^{-1} = \frac{\eta}{c} + \frac{\alpha\tau^2}{2\pi g(0)} \int_{-\infty}^{+\infty} \frac{g(\Delta\omega)d\Delta\omega}{1 + (\Delta\omega\tau)^2}, \quad (10)$$

which reduces to $V^{-1} \cong \alpha\tau/2$ for $T_2^* \ll \tau$ and $\alpha\tau \gg \eta/c$. The special results (8)-(10) are valid for nonsymmetric $g(\Delta\omega)$ if k in Eq. (1) is replaced by

$$k' = k + \frac{\alpha\tau^2}{2\pi g(0)} \int_{-\infty}^{+\infty} \frac{\Delta\omega g(\Delta\omega)d(\Delta\omega)}{1 + (\Delta\omega\tau)^2}. \quad (11)$$

In actual practice the light pulse enters a sample with nonuniform intensity across the beam. Any small portion of the wave front can be assumed to obey the predictions of the plane-wave model above for short distances. Small cross sections of the beam will tend to develop and maintain the 2π condition. Consequently, the more intense portions of the beam will exhibit shorter pulse delay times, and less intense portions will exhibit longer delay times. Diffraction effects neglected here will become important after some distance of propagation, particularly in those regions of the beam which become sharply collimated.

Assuming phenomenological damping terms added to Eq. (2) in a manner following Bloch,³ we find for $T_2^* \ll \tau \ll T_2', T_1$ and symmetric

$g(\Delta\omega)$ that

$$\frac{d\tau}{dz} = -\frac{4\pi}{3} N \hbar \omega g(0) \left(\frac{1}{T_1} + \frac{1}{T_2'} \right), \quad (12)$$

where T_1 is the energy-damping time constant, and the pulse energy per cm^2 is given by

$$\tau = \frac{\eta c}{4\pi} \int_{-\infty}^{\infty} \mathcal{E}^2 dt. \quad (13)$$

The constant loss rate is proportional to the product of the pulse delay time $\alpha\tau/2$ per unit sample length and the fraction T_2^*/τ of the ions excited. The pulse is assumed to deviate only slightly from the form (8) for a plane wave, and diffraction effects are neglected. However, the dependence of k' on τ in Eq. (11) (and, therefore, the pulse intensity) indicates the existence of an instability effect similar to self-focusing⁷ for ω applied to the high-frequency side of the

resonance line. The reverse focusing tendency should occur on the low-frequency side.

Some predictions of the above plane-wave model are qualitatively confirmed by initial experiments we have carried out on a liquid-helium-cooled ruby-rod sample (0.05% Cr^{+3} in Al_2O_3) of $\frac{1}{2}$ in. diam, $2\frac{3}{4}$ in. length, and $T_2^* \sim 10^{-10}$ sec. A Q-switched liquid-nitrogen-cooled ruby laser served as a pulse source which was suitably controlled to provide only the plane-polarized $\bar{E}(2E) \leftarrow 4A_2(\pm\frac{3}{2})$ output⁸ laser line. By thermal tuning this transition was resonant with the $4A_2(\pm\frac{1}{2}) \leftarrow \bar{E}(2E)$ transition of the sample with its optical C axis in the z direction. Input energies for delay experiments were about 3 mJ for 10-nsec pulses; and for transmission threshold studies a maximum pulse energy of about 5 mJ in 20 nsec was applied.

Figure 2 illustrates the nonlinear transmis-

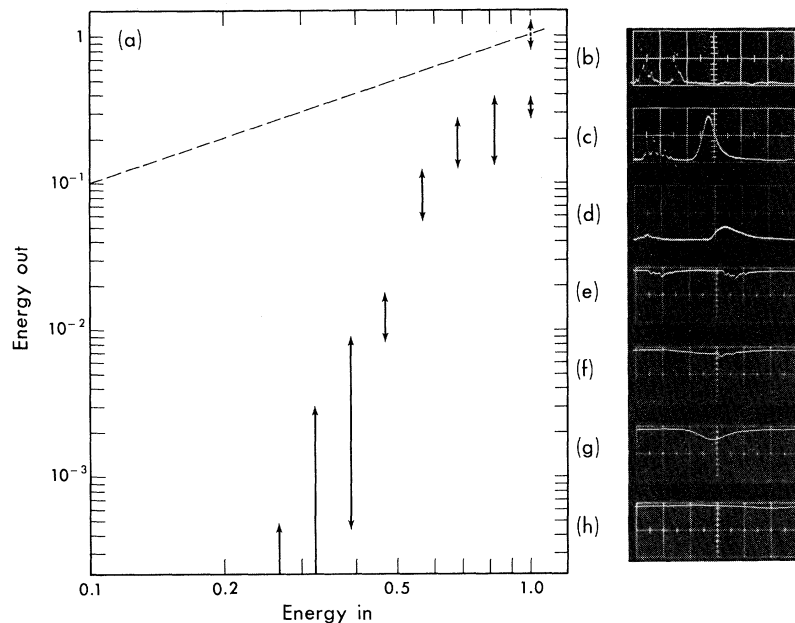


FIG. 2. (a) Energy output versus input ruby-light transmission through sample (arbitrary units). The magnified ($\times 14$) output is attenuated until Polaroid type-47, 3000 speed film is unexposed, thus determining peak transmitted energy/ cm^2 . Error bars represent output fluctuations presumably caused by several uncontrolled characteristics of the ruby-laser source and the finite steps in the output calibrated attenuation. The dotted datum is the transmission with the sample at room temperature, and the dashed line represents a linear transmission law. (b) Input and output laser pulses with sample at room temperature. An optical delay served to separate the two pulses. The second pulse has traveled through the sample. Sweep speed is 20 nsec per division with signal from a ITT Model FW-114 vacuum photodiode. (c), (d) Same as (b) except that the sample is thermally tuned by cooling to liquid helium and a $\times 20$ attenuator in output beam path is removed. (e) Output and input pulses with sample at room temperature. Here the first pulse is the output, and a semiconductor photodiode (Philco L-4501) of small sensitive area is used. Sweep speed is 10 nsec per division. (f) Same as (e) except a $\times 20$ output attenuator is removed and the sample is thermally tuned by cooling to liquid helium temperature. The delay in the resonant sample was sufficient to cause output and input to overlap. (g), (h) Same as in (f), except the input reference pulse is deleted, showing greater delay with increased width of the output pulse.

sion for various input intensities. Weak light, well below the onset of nonlinear transmission, was attenuated by more than 10^5 . The transmission reveals a reduction of $\sim 10^4$ in output pulse energy for a factor of 6 in the input attenuation. The anomalous transmission diminishes with increasing sample temperature, disappearing completely at 40°K , where the rapid Orbach relaxation⁹ between the upper levels $2\bar{A}(2E) \rightarrow \bar{E}(2E)$ imposes the condition $T_2' \lesssim \tau_p$. At the same time the thermal shift of the optical resonance only amounts to about $\frac{1}{4}$ of a linewidth,¹⁰ and the light is nearly completely attenuated. A large time delay and reshaping of the transmitted pulse through the sample is observed relative to the input pulse, as seen in Fig. 2. The delayed pulses are qualitatively in accord with Eq. (10), where the delay increases with pulse width τ . The larger delays correspond to increases in optical path lengths of about 100 sample lengths, in the absence of Cr^{+3} ions.

The nonlinear transmission behavior might be interpreted as a "hole-burning" effect in which the absorption line is simply saturated by the leading edge of the pulse. The factors arguing against such a possibility are chiefly that a population rate-equation description of these observations is not valid because damping times are long at liquid-helium temperatures in ruby; and the large pulse-delay times cannot be predicted by a rate-equation model.

We stress that the above experimental and theoretical observations at present are far from being well understood in terms of the actual experimental conditions. For example, either losses associated with T_2' or diffraction could account for the lack of sharpness in the knee of Fig. 2. Some complications to be considered are as follows: phase shifts and multiple modes in the incident laser pulse; diffraction and focusing properties of the evolving pulse in the resonant medium; evolution of the input pulse towards the ideal hyperbolic secant shape for nonsymmetric excitation of the $g(\Delta\omega)$ spectrum; and relation of the output pulse shape to T_2' .

The transmission effect is applicable as well to any two-level system, involving magnetic or electric multipole transitions which are resonant to traveling waves in the form of radio-frequency, microwave-frequency, or phonon pulse power.

We wish to thank the Advanced Research Project Agency for a single grant in partial support of apparatus purchases for this work. One of us (S.L.M.) wishes to thank the National Science Foundation for Fellowship support during part of this work. We thank M. Bass, L. Riley, and Y. R. Shen for helpful discussions.

*Work supported by the National Science Foundation.

†Submitted in partial fulfillment of the requirements for the degree of Doctor of Philosophy, Department of Physics, University of California, Berkeley, California.

‡Professor, Miller Institute for Basic Research in Science.

¹S. L. McCall and E. L. Hahn, *Bull. Am. Phys. Soc.* **10**, 1189 (1965).

²R. P. Feynman, F. L. Vernon Jr., and R. W. Hellwarth, *J. Appl. Phys.* **28**, 49 (1957); E. T. Jaynes and F. W. Cummings, *Proc. IEEE* **51**, 89 (1963); L. W. Davis, *Proc. IEEE* **51**, 76 (1963); I. D. Abella, S. R. Hartmann, and N. A. Kurnit, *Phys. Rev.* **141**, 391 (1966); C. L. Tang and B. D. Silverman, in *Physics of Quantum Electronics*, edited by P. L. Kelley, B. Lax, and P. E. Tannenwald (McGraw-Hill Book Company, New York, 1966), p. 280.

³F. Bloch, *Phys. Rev.* **70**, 460 (1946).

⁴Generally any combination of σ_{\pm} and π optical transitions may be handled by this model. For simplicity we consider only the behavior of moment \vec{P} induced by one circularly polarized component $\mathcal{E}(z, t)$.

⁵For a different physical situation occurring only in the time domain, E. T. Jaynes (private communication) finds that the hyperbolic secant function describes the electric field spontaneously emitted from a classically self-damped system which starts from $\theta \sim \pi$. R. H. Dicke, *Phys. Rev.* **93**, 99 (1954), using radiation damping arguments, obtains the same time function, with the system starting from $\theta = \pi/2$.

⁶This solution would apply to any magnetic moment $\vec{M}(\Delta\omega)$ in a magnetic resonance pulse experiment where the imposed rf cavity pulse field $H_1(t)$ is of the form of Eq. (8).

⁷R. Y. Chiao, E. Garmire, and C. H. Townes, *Phys. Rev. Letters* **13**, 479 (1964); G. A. Askarjan, *Zh. Eksperim. i Teor. Fiz.* **42**, 1567 (1962) [translation: *Soviet Phys.-JETP* **15**, 1088 (1962)]; V. I. Talanov, *Izv. Vysshikh Uchebn. Zavedenii Radiofiz.* **7**, 564 (1964).

⁸S. Sugano and Y. Tanabe, *J. Phys. Soc. Japan* **13**, 880 (1958).

⁹M. Blume, R. Orbach, A. Kiel, and S. Geschwind, *Phys. Rev.* **139**, A314 (1965); S. Geschwind, G. E. Devlin, R. L. Cohen, and S. R. Chin, *Phys. Rev.* **137**, A1087 (1965).

¹⁰D. E. McCumber and M. D. Sturge, *J. Appl. Phys.* **34**, 1682 (1963).

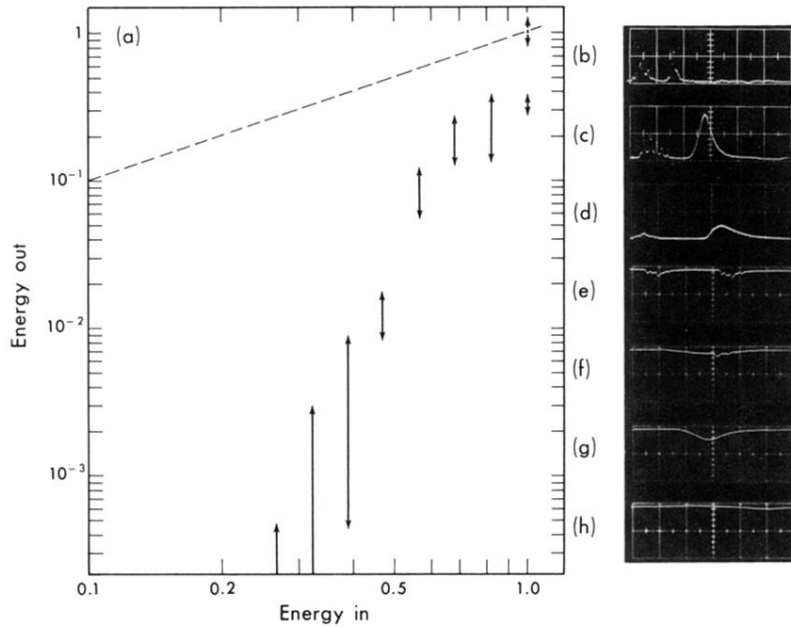


FIG. 2. (a) Energy output versus input ruby-light transmission through sample (arbitrary units). The magnified ($\times 14$) output is attenuated until Polaroid type-47, 3000 speed film is unexposed, thus determining peak transmitted energy/cm². Error bars represent output fluctuations presumably caused by several uncontrolled characteristics of the ruby-laser source and the finite steps in the output calibrated attenuation. The dotted datum is the transmission with the sample at room temperature, and the dashed line represents a linear transmission law. (b) Input and output laser pulses with sample at room temperature. An optical delay served to separate the two pulses. The second pulse has traveled through the sample. Sweep speed is 20 nsec per division with signal from a ITT Model FW-114 vacuum photodiode. (c), (d) Same as (b) except that the sample is thermally tuned by cooling to liquid helium and a $\times 20$ attenuator in output beam path is removed. (e) Output and input pulses with sample at room temperature. Here the first pulse is the output, and a semiconductor photodiode (Philco L-4501) of small sensitive area is used. Sweep speed is 10 nsec per division. (f) Same as (e) except a $\times 20$ output attenuator is removed and the sample is thermally tuned by cooling to liquid helium temperature. The delay in the resonant sample was sufficient to cause output and input to overlap. (g), (h) Same as in (f), except the input reference pulse is deleted, showing greater delay with increased width of the output pulse.